Inhibitors of nicotinamide phosphoribosyltransferase (NAMPT) cause retinal damage in larval zebrafish

Running title: NAMPT inhibitors damage zebrafish retina

Steven Cassar*,#, Christina Dunn*, Amanda Olson†, Wayne Buck*, Stacey Fossey*, Meg Ferrell Ramos*, Pankajkumar Sancheti†, DeAnne Stolarik†, Heather Britton‡, Todd Cole§, Natalie Bratcher¶, Xin Huang‖, Richard Peterson*, Kenton Longenecker111, and Bruce LeRoy*

*Preclinical Safety, AbbVie, North Chicago, Illinois, 60064, †DMPK, AbbVie, North Chicago, Illinois, 60064, ‡Comparative Medicine, AbbVie, North Chicago, Illinois, 60064, §Integrated Science and Technology, AbbVie, North Chicago, Illinois, 60064, ¶Global Animal Welfare, AbbVie, North Chicago, Illinois, 60064, ‖Statistics, AbbVie, North Chicago, Illinois, 60064, 111Discovery Chemistry and Technology, AbbVie, North Chicago, Illinois, 60064

To whom correspondence should be addressed. Phone: (847) 937-9302, E-mail: steven.cassar@abbvie.com, 1 North Waukegan Rd., North Chicago, Illinois, 60064.

Abstract

Nicotinamide phosphoribosyltransferase (NAMPT) has been investigated as a target for oncology because it catalyzes a rate-limiting step in cellular energy metabolism to produce nicotinamide adenine dinucleotide. Small molecule inhibitors of NAMPT have been promising drug candidates but preclinical development has been hindered due to associated retinal toxicity. Here we demonstrate that larval zebrafish can predict retinal toxicity associated with this mechanism revealing an attractive alternative method for identifying such toxicities. Zebrafish permit higher throughput testing while using far lower quantities of test article compared to mammalian systems. NAMPT inhibitor-associated toxicity manifested in zebrafish as a loss of response to visual cues compared to auditory cues. Zebrafish retinal damage associated with NAMPT inhibitor treatment was confirmed through histopathology. Ranking six NAMPT inhibitors according to their impact on zebrafish vision revealed a positive correlation with their *in vitro* potencies on human tumor cells. This correlation indicates translatable pharmacodynamics between zebrafish and human NAMPT and is consistent with on-target activity as the cause of retinal toxicity associated with NAMPT inhibition. Together, these data illustrate the utility of zebrafish for identifying compounds that may cause ocular toxicity in mammals, and, likewise, for accelerating development of compounds with improved safety margins.

Introduction

Studies uncovering the reliance of tumor cells on distinct energy metabolism pathways have delivered novel and promising cancer targets (Boroughs and DeBerardinis, 2015; Marin de Mas *et al*., 2014). Nicotinamide phosphoribosyltransferase (NAMPT) is overexpressed in many tumor

cells which rely upon it for the production of nicotinamide adenine dinucleotide (NAD), a key metabolite for sustaining energy metabolism. This makes NAMPT an attractive drug target for oncology indications (Bi and Che, 2010; Sampath *et al*., 2015). However, recent reports have demonstrated side effects associated with NAMPT inhibitor treatments in non-neoplastic tissues such as platelets, skin, gastrointestinal tract, and retina; these toxicities have arrested the development of promising therapeutics that use this mechanism (Sampath *et al*., 2015; Zabka *et al*., 2015).

NAMPT is expressed in all non-neoplastic tissues surveyed to date from dog, rat, and human (Duarte-Pereira, S., *et al*., 2015; McGlothlin *et al*., 2005; Samal *et al*., 1994; Zabka *et al*., 2015) and is an essential gene in mice, as evidenced by non-conditional and conditional knockout models (Zhang, *et al*., 2017). While NAMPT is apparently ubiquitously expressed, some tissues, like retina, are more sensitive to NAMPT inhibition. This may be due to a relatively high reliance on NAMPT for NAD synthesis. NAD can be synthesized by two major pathways which use different substrates (Bogan and Brenner, 2008; Wilsbacher *et al*., 2017). One pathway is driven by NAMPT activity, the other relies on nicotinic acid phosphoribosyltransferase (NAPRT1). Depending on relative gene expression and substrate availability, tissues may differ in their reliance on NAMPT versus NAPRT1 for NAD synthesis. Quantitative PCR analysis of NAMPT and NAPRT1 transcripts in 8 rat tissues revealed that retina expressed relatively high levels of NAMPT, and had a NAMPT-to-NAPRT1 ratio greater than 1, suggesting a higher reliance on NAMPT for NAD synthesis in retina (Zabka *et al*., 2015).

Recently we reported on the pharmacology of substrate and non-substrate inhibitors of NAMPT (Curtin *et al*., 2017; Wilsbacher *et al*., 2017). Non-substrate inhibitors are not phosphoribosylated by NAMPT, making them a new class of inhibitors. Given the reported

reliance of mouse vision on NAMPT activity (Lin *et al*., 2016) and the retinal toxicity associated with NAMPT inhibition (Zabka *et al*., 2015), we investigated effects on larval zebrafish vision in early toxicological assessment of one substrate and six non-substrate NAMPT inhibitors. This investigation allowed for *in vivo* assessment of retinal toxicities on an *in vitro* scale.

Zebrafish offer opportunities for higher throughput experiments and lower costs compared to mammalian models owing to their ease of handling, rapid development, and small size. The latter attribute is especially demonstrated by larval zebrafish. Larval zebrafish can survive for multiple days in small volumes of static water. As such, hundreds of larval zebrafish can be tested in simple multi-well plate formats using very small quantities of test compound. Where translatable biology is anticipated, this is an attractive platform for testing candidate compounds in early drug discovery; typically, large amounts of early discovery compounds are not readily available.

For zebrafish, visual development is rapid, with the behavior of free-swimming larvae becoming heavily reliant on visual cues by 4 days post-fertilization (dpf) (Easter and Nicola, 1996). By 3 dpf, although the retina is not yet fully mature, retinal neurogenesis is essentially complete, major retinal cell classes are detectable and organized into distinct layers, and ganglion cell axons have innervated the optic tectum (Avanesov and Malicki, 2010). Mammalian and zebrafish retinal organization, cell composition and gene expression patterns are similar (Avanesov and Malicki, 2010; Goldsmith and Harris, 2003; Slijkerman *et al*., 2015). All major cell types and tissue layers in mammalian retina are represented in zebrafish retina, including retinal nerve fiber layer, ganglion cell layer, inner plexiform layer, inner nuclear layer, outer plexiform layer, outer nuclear layer, inner and outer segments, and pigmented epithelium (Avanesov and Malicki, 2010; Slijkerman *et al*., 2015). Zebrafish have color vision like that of

humans, and their retina is correspondingly cone-dense. Alternatively, the mouse and rat, being nocturnal animals, have relatively fewer cones and poor color vision (Goldsmith and Harris, 2003).

Structural or cellular attributes of zebrafish retinas distinguishing them from mammalian retinas are that they lack a cone-rich area, have more cones than rods, possess ultraviolet-sensitive cones in addition to those for red, green, and blue, and have double cones composed of a principle (red) and an accessory (green) cone (Slijkerman *et al*., 2015). Perhaps the most significant difference between zebrafish and mammalian retina, and pertinent to using zebrafish to model retinal injury, is the regenerative capacity of zebrafish retina. This capacity, found in developing and mature retinas, relies on Müller glial cells which respond to injury by dividing to produce a retinal progenitor capable of generating all major retinal neuron types (Wan and Goldman, 2016).

Retinal angiogenesis and vasculature are similar between zebrafish and mammals. In both model systems, angiogenesis from a central retinal artery forms the retinal vasculature, and early hyaloid vasculature associated with the lens diminishes with age, leaving vasculature associated with the ganglion cell layer that persists into adulthood (Alvarez *et al*., 2007). In mature mammalian retinas, however, vessels branch to form intra-retinal capillaries that nourish the inner and outer plexiform layers. These capillaries are not present in adult zebrafish; presumably the thinner zebrafish retina needs fewer capillaries and can rely on diffusion from the surface (hyaloid and choroid) vessels (Alvarez *et al*., 2007).

Taken together with their ease of handling, rapid development, and small size, translational retinal biology gives the zebrafish an advantage as a highly relevant species for modeling

genetically- or pharmacologically-driven retinal degeneration, as evidenced in the literature (Deeti *et al*., 2014; Morris, 2011). Here we report the utilization of zebrafish larvae to assess retinal toxicities associated with NAMPT inhibitor treatment.

Methods

Animal husbandry

Adult wild-type zebrafish (*Danio rerio*) were housed in a continual-flow housing system (Tecniplast™ ZebTEC®). Water conditions were maintained by a centralized monitoring system and held constant at: temperature 28±1°C, pH 7.5±0.5, conductivity 950 microsiemens. General husbandry and breeding were conducted using standard conditions (Westerfield, 2000). Embryos were collected from breeding tanks 2-3 hours after removing the male/female separation barrier. Larval fish were housed in 10 cm petri dishes (50 fish/50 ml) and kept in an incubator on a 14:10 light:dark cycle at 28±1°C. Larval fish water (pH = 7±0.5) was 60 µg/ml Instant Ocean™ Sea Salts. At the end of experiments, zebrafish were humanely euthanized in 4°C water. All experiments were conducted in compliance with AbbVie's Institutional Animal Care and Use Committee (IACUC). AbbVie operates under the National Institutes of Health Guide for Care and Use of Laboratory Animals in a facility accredited by the Association for the Assessment and Accreditation of Laboratory Animal Care (AAALAC).

Compounds

Seven small molecule inhibitors of human NAMPT were tested for their effects on zebrafish vision (Fig. 1). Only one of these compounds, the azaisoindoline A-1326133, is a phosphoribosylated substrate of NAMPT, while the other 6 compounds are members of the isoindoline series and are non-substrate inhibitors of NAMPT (Curtin *et al*., 2017; Wilsbacher *et*

al., 2017). These seven compounds were chosen because, as a group, they exhibit a range of *in vitro* inhibitory potencies on human tumor cell proliferation (Fig. 1) and therefore represent a relevant test set to explore a potential range of effects on zebrafish vision.

Maximum Tolerated Dose

To determine an appropriate concentration range for each test compound in the vision assays, a maximum tolerated dose (MTD) study was performed. Compound solutions were prepared as described below for vision assays. The 7-concentration dilution series for each compound ranged from 0.3 μM to 300 μM at ½-log intervals. To prevent clutch-specific or genetic deficiencies from impacting the identification of treatment-specific effects, all treatments within a given experiment, including vehicle control, contained equal numbers of fish from the same clutches. Five dpf zebrafish were exposed to treatments for 48 hours at 28±1°C in 24-well plates (6 fish per well). Each well contained 2 ml of a different concentration of the test compound dilution series, and each plate contained a vehicle-treated (0.3% dimethyl sulfoxide) control group. Fish were then evaluated for survival using a dissecting stereoscope or compound microscope. Mortality was confirmed visually by absence of heartbeat. Sub-lethal toxicity was qualitatively assessed by lack of startle response to a tactile stimulus (gentle touch on the dorsal surface with a fine pipette tip) or the presence of a gross morphological abnormality, such as pericardial or whole body edema. The MTD was defined as the highest concentration that did not cause death and did not induce sub-lethal toxicity.

Vision Assays

Test compounds were solubilized as 300x stocks in dimethyl sulfoxide (DMSO) and administered in larval fish water at 3 concentrations: high (same as MTD), middle (½-log below

MTD), and low (½-log below middle) (see Table 1). The DMSO concentration was 0.3% for each treatment, including the vehicle treatment. Compound solution pH was measured and, when necessary, titrated to pH 7.0 using sodium bicarbonate or hydrochloric acid. As was done for the MTD studies, all treatments within a given experiment, including vehicle control, contained equal numbers of fish from the same clutches. Treatments were administered to fish starting on day 5 post-fertilization for a total of 72 hours; the dosing solution was replenished with fresh dosing solution after the first 48 hours, to maintain continued exposure levels for the final 24 hours. Twelve fish were used in each treatment group, being held together in a single well of a 12-well plate in a volume of 2 ml. Each compound was accompanied by a designated vehicle-treated group of 12 fish.

Startle response

Startle response in larval zebrafish is defined as any abrupt movement occurring within 2 seconds of a light or sound stimulus (Bhandiwad *et al*., 2013; Portugues and Engert, 2009; Scott *et al*., 2016). After the 72 hour treatment with the experimental molecules, startle responses to light and sound stimuli were quantified using a behavioral tracking system as follows. While still in the 12-well plate used for dosing, the fish were acclimated to the dark for 5 minutes in a behavioral tracking device (ZebraBox®; Viewpoint™). Then ensued three 5-second periods of light (20% intensity), each separated by 1 minute of darkness. The light remained on after the third period for the remainder of the assessment, during which fish were exposed to three 40-milliseconds of sound (660 Hertz) each separated by 1 minute of silence. The total activity for each treatment was quantified using ZebraLab® software (Viewpoint™). An activity integral, representing the sum of all image pixel changes detected within the well for each 1 second period of the program was computed and recorded by the software.

To generate a startle response metric, the average activity per second during the 25 seconds immediately prior to a stimulus was subtracted from the activity ensuing during the 1-second period following the start of the stimulus. Thus the value represents the startle response as a difference from background for each stimulus. These data are expressed as % vehicle-treated response.

Optomotor response

After recording startle responses, fish were tested in an optomotor response (OMR) assay. This assay relies on directional swimming prompted by visual cues (stripes of contrasting color, moving independently of the subject in a constant direction for a prescribed period of time) (Berghmans *et al*., 2008, Maaswinkel and Li, 2003). Healthy fish swim in the same direction as the pattern moves. We conducted the optomotor response assay as follows. Fish treated with vehicle, low, middle, and high doses for a given test compound were transferred to a clear acrylic manifold into separate parallel troughs, each measuring 26 x 1 x 1 centimeters. These troughs contained 15 ml of treatment solution to maintain exposure. The manifold was placed on a computer monitor. A visual stimulus (Carpetbones™; https://carpetbones.itch.io/zot) was displayed, consisting of black and white alternating stripes, 2 centimeters wide, spanning the monitor, and moving perpendicular to the length of the troughs at a speed such that the black/white pattern replaced itself every 2.5 seconds (stripes moving at 1.6 centimeters/second). The stimulus first moved one direction for 3 minutes, after which fish located in the final ¼ (6.5 cm) of the trough were counted. Then the stimulus moved in the opposite direction for 3 minutes, and fish were counted in the opposite ¼ of the trough. These trials were repeated two more times for a total of 6 trials, 3 each direction.

OMR data are presented as the percent of fish found in final ¼ of trough (i.e. passing the assay), expressed as an average of the 6 trials. Comparison to the vehicle group was performed via a Student's t-test of the 6 trials. In order to fail the assay, a group had to have a pass average significantly lower than that of the vehicle group, and below 52.3%. This value (52.3%) represents the lower 10^{th} percentile of 126 trials of vehicle groups tested on this platform. The use of this qualification rule is estimated to keep the false positive rate of this assay at or below 10%. An assay was invalidated if the vehicle group pass average did not exceed 52.3%.

Histopathology

After the OMR assay, three fish from each treatment, as well as from the vehicle control group were euthanized in 4°C water and transferred individually to 1.5 ml conical vials containing 0.5 ml of 10% neutral buffered formalin. These fish were kept at room temperature at least overnight, and then prepared for sectioning as follows. Fish were embedded cranial side down in a 2% agarose matrix to maintain their orientation as well as to enable processing for paraffin embedding. These fish were then processed through a series of graded alcohol and xylene concentrations, and infiltrated with melted paraffin following standard histology processing protocol. Whole fish were embedded in paraffin cranial side down to enable microtomy sectioning of the head within a transverse plane. Serial sections, 4 µm thick, were taken from rostral to caudal to capture all features of the eye. The sections were placed on positive charged glass slides and routine H&E staining was performed. Sections were examined using an Olympus BX41 light microscope and images were acquired using an Olympus DP72 camera.

Larval fish treated with 30 µM A-1326133 for 3 days were collected for transmission electron microscopy (TEM) of the retina. This compound/dose was chosen for TEM assessment of retinal

damage based on results from the initial experiment which tested only A-1326133 and A-1293201. In that experiment, 30 μM A-1326133 was the most toxic treatment on zebrafish vision and had the most evident retinal findings by H&E staining. After euthanasia in 4°C water, treated fish were collected, along with vehicle-treated fish individually into 1.5 ml vials containing 0.5 ml of ½ strength Karnovsky's fixative in 0.1 M Sorensen's phosphate buffer (SPB) pH 7.2-7.4 and stored at 4°C for at least 24 hours. The fish were then washed in two exchanges of 0.1 M SPB pH 7.3 prior to post-fixing in 1% osmium tetroxide in 0.1 M SPB for 1 hour at room temperature (RT). Osmium tetroxide was removed and replaced with 0.1M SPB, which was replaced with deionized water (15 min each at RT). Fish were then dehydrated at RT through a graded ethanol series, 50%, 75% (one exchange each for 15 min), 95% (two 15 min exchanges), and 100% (two 10 min exchanges). Ethanol was cleared using propylene oxide (two 10 min exchanges), followed by overnight incubation in 1:1 propylene oxide: epoxy resin, which was replaced with 100% epoxy resin. Fish were embedded in flat silicon molds in 100% epoxy resin and polymerized at 60°C for 4 days.

Semi-thin 1 μm sections of the fish were prepared using an EM UC6 ultra microtome (Leica Microsystems™) and stained on glass slides with 1% toluidine blue/sodium borate. Ultrathin ~80 nm sections were prepared from selected blocks based on evaluation of the toluidine-blue slides, collected on 3 mm, 200 mesh, Cu/Rh grids and stained with 2% methanolic uranyl acetate followed by Reynold's lead citrate. Ultrathin sections were viewed and images were acquired using a JEM1400 TEM (JEOL™) operated at 80 kV equipped with an AMT XR-41 digital camera (Advanced Microscopy Techniques™).

Drug Analysis

After the OMR assay, three fish from each treatment group were euthanized in 4°C water, rinsed in 50 ml of larval fish water two times and placed together into a pre-weighed vial. The majority of water was then carefully removed and the vial placed in dry ice. After determining the mass of the 3 fish, deionized water (300 µl) was added and they were homogenized using an Omni Bead Ruptor 24® (Omni International™). An aliquot of fish homogenate and set of standards were pipetted into a 96-well plate and subjected to protein precipitation extraction on Microlab Star robot® (Hamilton Robotics™). The dosing solutions were likewise prepared. A dilution series was made to generate a range of standards from 1000 ng/ml to 0.1 ng/ml. The acetonitrile, containing 6 reference compounds (12.5 nM verapamil, 1000 nM dexamethasone, 200 nM diclofenac, 250 nM carbutamide, 125 nM lidocaine, and 100 nM tolbutamide) as internal standards, was used as an organic solvent to precipitate out all the biological proteins from fish and dosing solution. Supernatant from protein precipitation was transferred into mass spectrometry plates and diluted with the mobile phase of the liquid chromatography–mass spectrometry (LC-MS) column. The liquid chromatography analysis was performed using reverse phase or HILIC chromatography in either positive or negative ion mode using gradient elution. The tandem mass spectrometry analysis was carried out on SCIEX™ triple quadrupole mass spectrometer with an electrospray or atmospheric pressure ionization interface. Data acquisition and evaluation were performed using Analyst® software (SCIEX™).

For comparing drug levels of a NAMPT inhibitor in the eye with that of the rest of the body, 10 month old zebrafish (n=3) were treated with 30 µM A-1326133 in fish system water (pH 7.0, 920 µS, 28°C), or vehicle (system water plus 0.3% DMSO) for 3 days. After this period, following euthanasia in 4°C water, the eyes were dissected from the remainder of the body. Drug analysis was performed as described above, treating eyes and body separately.

Calculation of Zebrafish Vision Loss 50 (VL50)

To allow for comparing toxic potencies of test compounds on zebrafish vision, we devised a zebrafish % Vision Loss-50 index (VL50). The VL50 is a prediction of the amount of test compound required in the larval fish to drive a 50% deficit in the startle response to light as compared to vehicle-treated fish. The VL50 was derived by the following method: startle responses to light (as % vehicle) were plotted as a function of the amount of compound measured in the fish (pmoles per larva) for each dose level. A linear regression was generated for each compound using those points, and including a point representing vehicle (100% and 0 pmoles/larva). Using that regression equation, the value of x where y=50 was calculated. This represents the level of compound in the fish predicted to drive a 50% deficit in the startle response to light, and is the VL50.

Alignment and 3D modeling of human and zebrafish NAMPT activation site

A structural model of the zebrafish NAMPT protein was constructed from the predicted sequence recorded with NCBI reference number XP_002661386 using the homology modeling module within the Maestro suite® (Schrodinger™). The crystal structure of human NAMPT in complex with inhibitor A-1326133 (pdb code 5U2N) was used as basis for the model of the protein structure. The final image was prepared using the program PyMOL® (Schrodinger™).

Results

Drug analysis and Maximum Tolerated Dose

The average solubility for all treatments analyzed was 50.4% (±19.3). Solubility was calculated by dividing the dose solution concentration, as measured by LC-MS (data not shown), by the

target concentration for each treatment. All NAMPT inhibitors were well absorbed by the larval fish. The average absorption for all treatments was $1.9x10^{-6}$ (μmoles per larva / μM in dose solution). For perspective, absorption values from all treatments in this report were in the upper 25% of that for 43 drugs in our prior report (Cassar *et al*., 2017). Compound levels detected in larvae were dose-dependent for all 7 compounds; increasing the dose increased levels in the fish (Table 1). These data were used to build dynamic relationships between compound exposure and behavioral endpoints, and for calculating VL50s. Maximum tolerated doses ranged from 3 to 300 μM. For each compound, the highest dose listed in Table 1 was the MTD. Concentrations above the MTD resulted in mortality of ≥ 2 fish and/or in loss of response to touch for ≥ 3 fish (out of 6). Loss of response to touch was considered a severe finding since those fish would likely not respond to a visual stimulus, regardless of retinal function. As such, the MTD is the concentration where at least 5 of 6 fish survived, and at least 4 of 6 responded to touch. Besides the loss of response to touch, there were no other sub-lethal toxicities noted.

Providing a tissue distribution basis for vision liability, levels of A-1326133 in the eyes of adult fish were, on average, 4.9 (± 2.3) times higher than that detected in the rest of the body (mass/volume), demonstrating that this compound can accumulate in the eye of zebrafish.

Vision Assays

Startle response

Among vehicle-treated groups, the standard deviations for startle responses to light and sound, calculated as percent of the average, were 67% and 52% respectively (data not shown). Expressing data from compound-treated groups as percent of vehicle response allowed for detecting dose-related effects despite this high variability. Startle response to light was impacted

by NAMPT inhibitors in a concentration-dependent manner (Table 1). For 6 of the 7 compounds, the MTD ablated the startle response to light. Response to sound for the same groups was not ablated (Table 1, Fig. 2), indicating that the observed deficits in response to light are likely caused by loss of vision rather than by a general effect on mobility and/or the central nervous system. The only compound that did not ablate the startle response to light was A-1325236.

The exposure dependent loss in vision allowed for estimating the exposure necessary to drive a 50% loss in vision (VL50) for 6 of the 7 compounds. A-1325236 was not included because fish dosed with the MTD did not lose vision, maintaining a response to light. For the other 6 compounds, comparing VL50s to *in vitro* potencies on a human prostate cancer cell line (PC3) (see Wilsbacher *et al*., 2017 for methods) revealed a positive correlation ($R^2 = 0.45$, Fig. 3). This suggests an on-target mechanism for vision liabilities associated with NAMPT inhibition and indicates translatable pharmacology for these compounds between zebrafish and human. Comparison of the model of A-1326133 interacting with zebrafish NAMPT to the crystal structure of the same compound bound to human NAMPT reveals a high conservation of residues in the inhibitor binding site and suggests that amino acid differences in the zebrafish NAMPT are not likely to interfere with binding (Fig. 4).

Optomotor response (OMR)

Poor performance in the OMR correlated with NAMPT inhibitor exposure (Table 1). Failure rates were high, reflecting the relatively high doses tested (in the vicinity of the MTD). The OMR proved to be more sensitive to drug effects than that of the startle response. That is, some of the same groups with robust startle responses to light (≥ vehicle response) failed the OMR (Fig. 5).

Visual Background Adaptation, Histopathology, and Electron Microscopy

Larval fish dosed with high levels of some of the NAMPT inhibitors appeared grossly darker than fish in vehicle-treated and lower dosed cohorts. The dark appearance was derived from increased visible melanin in the skin (Fig. 6). In the melanophores of larval zebrafish, melanin-filled vesicles (melanosomes) are dispersed in response to low light levels, engendering a darkened camouflage; this is referred to as visual background adaptation (Logan *et al*., 2006). The observations of increased pigmentation in NAMPT-inhibitor-treated fish were made during lights-on periods, when vehicle treated fish were sparsely pigmented (Fig. 6). Loss of proper visual background adaptation in zebrafish has been associated with loss of retinal ganglion cells (Kay *et al*., 2001). Indeed, for fish dosed with 5 of 7 NAMPT inhibitors, examination of H&E stained tissue sections revealed retinal degeneration characterized by decreased numbers of nuclei in the ganglion cell layer and inner nuclear layer (Fig. 7). Increased clear space in these layers was attributed to loss of nuclei and disorganization. Reduced numbers of cell layers resulted in diminished height, collapse, and disorganization of these layers. Clear spaces within the inner plexiform and nerve fiber layers were increased and considered related to fewer axons and dendrites in these areas secondary to nuclei loss. The compounds not associated with such lesions were A-1466391 and A-1325236 (see Discussion).

Transmission electron micrographs of slides prepared from larval fish dosed with 30 μM A-1326133 revealed decreased cell density and neuronal death in the inner nuclear and retinal ganglion layers (Fig. 7). The neuronal death was characterized by condensation and fragmentation of chromatin, which is consistent with apoptosis. Apoptotic bodies (granular electron dense nuclear remnants) were present in the ganglion cell, inner plexiform and inner

nuclear layers. Vacuolation was also observed in the inner plexiform layer associated with this NAMPT inhibitor treatment, consistent with loss of cytoplasmic processes.

Two of the seven compounds from this report (A-1293201 and A-1326133) were tested in mammals. Similar to the NAMPT inhibitor associated toxicity reported by Zabka *et al.* (2015), these compounds caused retinal damage. For A-1326133, retinal toxicity was observed in dogs (data not shown) and rats. Figure 8 shows retinal damage in a rat dosed with 10 mg/kg A-1326133 once a day for a total of 8 days; the dose regimen, projected to provide efficacy while minimizing toxicity, was 4 days on, 3 days off, and 4 days on treatment. The damage is characterized by loss of photoreceptor nuclei and segments, loss and collapse of the outer plexiform layer and rarefaction and vacuolation of the inner plexiform layer. For A-1293201, similar findings were observed in corresponding cell layers of dog retina (data not shown).

Discussion

Monitoring drug solution concentrations and exposure levels in larval fish experiments can help interpret biological and behavioral endpoints (Cassar *et al*., 2017). Dose-related increases in exposure for NAMPT inhibitors were associated with total loss of response to visual cues at the MTD for most compounds. For each of the 7 compounds, exposure at the MTD was 2-4 times higher than that of the next lower dose (calculated from Table 1). This observation highlights the dose-exposure-toxicity relationship for these NAMPT inhibitors on retina and demonstrates the utility of this assay for prioritizing safe compounds above more toxic ones.

Factors that can influence relative toxicity include drug metabolism, potency on zebrafish NAMPT, as well as dose range, exposure, and biodistribution in zebrafish. Of these factors, only dose range and exposure were measured in these experiments. Having these values, and knowing

relative potencies on PC3 cells, allows for further interpretation of results. For example, A-1325236 appears safer than the others because it did not ablate response to light at its MTD. However exposure may have been too low given this compound's relative low potency on inhibiting PC3 tumor cell growth. Only A-1293201 and A-1343741 have weaker potencies on PC3 compared to A-1325236 (Fig. 1) and response to light was ablated by those 2 compounds only at higher levels than that achieved by A-1325236 (Table 1). Still, A-1459319, which has similar potency to A-1325236, ablated response to light at an exposure equal to that achieved by A-1325236. Some unexamined factors that could be playing a role in this discrepancy are relative potencies on zebrafish NAMPT and differences in biodistribution (eye penetration).

The only compound for which eye tissue concentrations were measured in this report was A-1326133. Due to the small size of larval zebrafish, this experiment was conducted in adult zebrafish. The high levels measured in the eyes versus the rest of the body for A-1326133, indicate that it accumulates in the eye. A-1326133 is phosphoribosylated by NAMPT. This change increases the polarity of the compound and decreases its ability to penetrate the cell membrane. In tissues with high NAMPT expression, substrate inhibitors of NAMPT (like A-1326133) may accumulate, being confined to the cell once phosphoribosylated. If zebrafish, like rat, express high levels of NAMPT in retinal cells, this could explain the higher concentrations of A-1326133 in the eye compared with the systemic exposure. The other compounds that caused vision loss and retinal damage may also accumulate in the eye, but perhaps to different extents. Comparing abilities of all compounds to penetrate zebrafish eyes may help interpret differences in toxic potency.

The limited data presented herein, suggests that non-substrate inhibitors of NAMPT, as a class, do not offer an advantage over the substrate inhibitor (A-1326133) in mitigating retinal toxicity.

However, a fully informative comparison would require matched pairs of compounds differing only in the presence or absence of the aromatic nitrogen capable of being phosphoribosylated by NAMPT. Without such direct comparisons, a decision on the benefit of non-substrate inhibitors for alleviating toxicity cannot be reached.

The comparable relative potencies of these NAMPT inhibitors in preventing PC3 growth and causing retinal damage in zebrafish larvae, together with the predicted structural homology of the inhibitor binding sites, indicate translatable pharmacology between zebrafish and human NAMPT. These data also indicate that mammalian retinal toxicities reported with this pharmacology are driven by an on-target mechanism. Namely, NAMPT inhibition in retinal cells likely decreases NAD to intolerable levels and results in cell death due to energy depletion.

Aside from the inner plexiform layer, the retinal layers impacted in mammals (photoreceptor and outer nuclear) are not homologous with the layers impacted in zebrafish larvae (ganglion cells and inner nuclear). Reasons for this incongruity are unknown. Some possible reasons are: differences in NAMPT versus NAPRT1 expression among retinal cell types between the two models which has yet to be explored; differences in vascularization, since zebrafish unlike mammals do not have intra-retinal capillaries (Alvarez *et al*., 2007) possibly explaining why those layers closest to retinal arteries in zebrafish are more susceptible; the stage of life, zebrafish larvae being at an earlier stage with a developing retina compared to adult mammals, which may cause differential energy requirements among cell layers; or from differences in dosing route, in-water dosing of zebrafish versus oral dosing of mammals.

It has been reported that apoptosis occurs in the ganglion cell layer and inner nuclear layer of larval zebrafish at low levels during early development (3-4 dpf) (Biehlmaier *et al.*, 2001). The

studies reported herein were conducted starting at 5 dpf, and apoptosis was not observed in vehicle-treated age-matched larvae. This suggests that apoptosis observed in connection with NAMPT inhibitors was not development related.

It is unknown if retinal regeneration influenced the visual or histopathological results of our experiments. Our methods ensured continual exposure of the larvae to the test compounds throughout visual testing and up to the time of euthanasia, preventing a recovery period. Also, the duration of treatment used herein (72 hours) is roughly the same time reportedly involved in cellular reprogramming and neuronal precursor generation (Gorsuch and Hyde, 2014; Kassen *et al*., 2007). These conditions suggest that, if any, only minimal effects from regenerative activity might be expected on the observed toxicities of these compounds.

The OMR assay detected toxicity in treatment groups where the startle response was not impacted. This highlights the influence of locomotion on OMR performance; not only do the fish need to see the visual stimulus but they must have the ability to swim nearly as well as vehicle-treated fish for the duration of the assay. It is reasonable to speculate that NAMPT inhibition, impacting energy metabolism, may adversely affect swimming ability in fish, in addition to vision. The startle response, because it is a quick, reflexive action that does not rely on endurance, may indicate retinal function with more specificity than the optomotor response.

Retinal degeneration was noted for 5 of the 7 NAMPT inhibitors. No retinal lesions were noted for fish treated with A-1466391 or A-1325236. Unlike A-1325236, treatment with A-1466391 resulted in exposure-related vision loss. The possibility exists that retinal damage had ensued but was not evident with light microscopic examination in tissue sections captured from those fish.

Impaired vision can occur in some retinal toxicities that impair electrophysiological function in absence of, or preceding, development of anatomical lesions (Ramos *et al.*, 2011).

Development of promising cancer therapies is often hampered by tissue specific toxicity. Retinal toxicity is a key toxic finding in preclinical testing of NAMPT inhibitors as reported here and elsewhere (Sampath *et al*., 2015; Zabka *et al*., 2015). Anatomy and physiology of the zebrafish retina are well characterized (Avanesov and Malicki, 2010; Goldsmith and Harris, 2003; Slijkerman *et al*., 2015). The many similarities in gene expression, cell composition, anatomical architecture, and function between zebrafish and mammalian retinas typify the conserved nature of the vertebrate eye. When translatable biology like this is anticipated, the zebrafish can be a powerful tool for drug development. This model offers significantly higher throughput and requires less test article than mammalian models. Zebrafish can be employed early in drug development to identify safer drug candidates, or to help discover successful mitigation strategies designed to alleviate the toxicity of promising chemotherapeutics on non-tumor cells.

Acknowledgments

The authors would like to thank the following for scientific advice and experimental support, Julie Wilsbacher, Chris Tse, Michael Curtin, Abby Turner, Belen Tornesi, Terry Van Vleet, Ronnie Yeager, James W. Rhodes, Julie Johnson, and Eric Blomme.

Disclosure

Financial support for these experiments was provided by AbbVie. AbbVie participated in the interpretation of data, review, and approval of the manuscript. All authors are employees of AbbVie and have no additional conflicts of interest to disclose.

References

1. Alvarez, Y., Cederlund, M. L., Cottell, D. C., Bill, B. R., Ekker, S. C., Torres-Vazquez, J., Weinstein, B. M., Hyde, D. R., Vihtelic, T. S., and Kennedy, B. N. (2007). Genetic determinants of hyaloid and retinal vasculature in zebrafish. *BMC Dev Biol*. **7**, 114-31.
2. Avanesov, A., and Malicki, J. (2010). Analysis of the retina in the zebrafish model. *Methods Cell Biol*. **100**, 153-204.
3. Berghmans, S., Butler, P., Goldsmith, P., Waldron, G., Gardner, I., Golder, Z., Richards, F. M., Kimber, G., Roach, A., Alderton, W., and Fleming, A. J. (2008). Zebrafish based assays for the assessment of cardiac, visual and gut function--potential safety screens for early drug discovery. *Pharmacol Toxicol Methods* **58(1)**, 59-68.
4. Bhandiwad, A. A., Zeddies, D. G., Raible, D. W., Rubel1, E. W., and Sisneros, J. A. (2013). Auditory sensitivity of larval zebrafish (Danio rerio) measured using a behavioral prepulse inhibition assay. *J Exp Biol*. **216**, 3504-13.
5. Bi, T., and Che, X. (2010). Nampt/PBEF/visfatin and cancer. *Cancer Biol Ther.* **10(2)**, 119-125.
6. Biehlmaier, O., Neuhauss, S. C., and Kohler, K. (2001). Onset and time course of apoptosis in the developing zebrafish retina. *Cell Tissue Res*. **306(2)**, 199-207.
7. Bogan, K. L., and Brenner, C. (2008). Nicotinic acid, nicotinamide, and nicotinamide riboside: a molecular evaluation of NAD+ precursor vitamins in human nutrition. *Annu Rev Nutr.* **28**, 115–30.
8. Boroughs, L. K., and DeBerardinis, R. J. (2015). Metabolic pathways promoting cancer cell survival and growth. *Nat Cell Biol*. **17(4)**, 351–359.
9. Cassar, S., Breidenbach, L., Olson, A., Huang, X., Britton, H., Woody, C., Sancheti, S., Stolarik, D., Wicke, K., Hempel, K., and LeRoy, B. (2017). Measuring drug absorption improves

interpretation of behavioral responses in a larval zebrafish locomotor assay for predicting seizure liability. *J Pharmacol Toxicol Methods* **88**, 56-63.

10. Curtin, M. L., Heyman, H. R., Clark, R. F., Sorensen, B. K., Doherty, G. A., Hansen, T. M., Frey, R. R., Sarris, K. A., Aguirre, A. L., and Shrestha, A. (2017). SAR and characterization of non-substrate isoindoline urea inhibitors of nicotinamide phosphoribosyltransferase (NAMPT). *Bioorg Med Chem Lett.* **27(15)**, 3317-3325.
11. Deeti, S., O'Farrell, S., and Kennedy, B. N. (2014). Early safety assessment of human oculotoxic drugs using the zebrafish visualmotor response. *J Pharmacol Toxicol Methods* **69**, 1–8.
12. Duarte-Pereira, S., Pereira-Castro, I., Silva, S. S., Correia, M. G., Neto, C., da Costa, L. T., Amorim, A., and Silva, R. M. (2015). Extensive regulation of nicotinate phosphoribosyltransferase (NAPRT) expression in human tissues and tumors. *Oncotarget* **7(2)**, 1973-83.
13. Easter, S. S., Jr., and Nicola, G. N. (1996). The development of vision in the zebrafish (Danio rerio). *Developmental Biology* **180**, 646–663.
14. Goldsmith, P., and Harris, W. A. (2003). The zebrafish as a tool for understanding the biology of visual disorders. *Seminars in Cell & Developmental Biology* **14**, 11–18.
15. Gorsuch, R. A., and Hyde, D. R. (2014). Regulation of Müller glial dependent neuronal regeneration in the damaged adult zebrafish retina. *Exp Eye Res*. **123**, 131-140.
16. Kassen, S. C., Ramanan, V., Montgomery, J. E., Burket, C. T., Liu, C., Vihtelic, T. S., and Hyde, D. R. (2007). Time course analysis of gene expression during light-induced photoreceptor cell death and regeneration in albino zebrafish. *Dev Neurobiol*. **67(8)**, 1009-31.
17. Kay, J. N., Finger-Baier, K. C., Roeser, T., Staub, W., and Baier, H. (2001). Retinal ganglion cell genesis requires lakritz, a zebrafish atonal homolog. *Neuron* **30**, 725–736.

18. Lin, J. B., Kubota, S., Ban, N., Yoshida, M., Santeford, A., Sene, A., Nakamura, R., Zapata, N., Kubota, M., Tsubota, K., *et al*. (2016). NAMPT-mediated NAD+ biosynthesis is essential for vision in mice. *Cell Rep*. **17(1)**, 69–85.

19. Logan, D. W., Burn, S. F., and Jackson, I. J. (2006). Regulation of pigmentation in zebrafish melanophores. *Pigment Cell Research* **19(3)**, 206-13.

20. Maaswinkel, H., and Li, L. (2003). Spatio-temporal frequency characteristics of the optomotor response in zebrafish. Vision Research **43**, 21–30.

21. Marín de Mas, I., Aguilar, E., Jayaraman, A., Polat, I. H., Martín-Bernabé, A., Bharat, R., Foguet, C., Milà, E., Papp, B., Centelles, J. J., and Cascante, M. (2014). Cancer cell metabolism as new targets for novel designed therapies. *Future Med Chem*. **6(16)**, 1791-810.

22. McGlothlin, J. R., Gao, L., Lavoie, T., Simon, B. A., Easley, R. B., Ma, S., Rumala, B. B., Garcia, J. G. N., and Ye, S. Q. (2005). Molecular cloning and characterization of canine pre-B-cell colony-enhancing factor. *Biochem Genet*. **43(3-4)**, 127-41.

23. Morris, A. C. (2011). The genetics of ocular disorders: insights from the zebrafish. *Birth Defects Res C Embryo Today*. **93(3)**, 215-28.

24. Portugues, R., and Engert, F. (2009). The neural basis of visual behaviors in the larval zebrafish. *Curr Opin Neurobiol*. **19(6)**, 644-47.

25. Ramos, M., Reilly, C. M., and Bolon, B. (2011). Toxicological pathology of the retina and optic nerve. In Fundamental Neuropathology for Pathologists and Toxicologists (B. Bolon and M. Butts, Eds.), 1st ed., pp. 385-412. John Wiley & Sons, Inc., Hoboken, NJ, USA.

26. Samal, B., Sun, Y., Sterns, G., Xie, C., Suggs, S., and McNiece, I. (1994). Cloning and characterization of the cDNA encoding a novel human pre-B-cell colony-enhancing factor. *Mol Cell Biol*. **14(2)**, 1431-7.

27. Sampath, D., Zabka, T. S., Misner, D. L., O'Brien, T., and Dragovich, P. S. (2015). Inhibition of nicotinamide phosphoribosyltransferase (NAMPT) as a therapeutic strategy in cancer. *Pharmacology & Therapeutics* **151**, 16–31.

28. Scott, C. A., Marsden, A. N., and Slusarski, D. C. (2016). Automated, high-throughput, in vivo analysis of visual function using the zebrafish. *Dev Dyn*. **245(5)**, 605-13.

29. Slijkerman, R. W., Song, F., Astuti, G. D., Huynen, M. A., van Wijk, E., Stieger, K., and Collin, R. W. J. (2015). The pros and cons of vertebrate animal models for functional and therapeutic research on inherited retinal dystrophies. *Prog Retin Eye Res* **48**, 137-59.

30. Wan, J., and Goldman, D. (2016). Retina regeneration in zebrafish. *Curr Opin Genet Dev*. **40**, 41-47.

31. Westerfield, M. (2000). The Zebrafish Book. A Guide for the Laboratory Use of Zebrafish (Danio Rerio). Eugene, OR: University of Oregon Press.

32. Wilsbacher, J. L., Cheng, M., Cheng, D., Trammell, S. A. J., Shi, Y., Guo, J., Koeniger, S. L., Kovar, P. J., He, Y., Selvaraju, S., *et al*. (2017). Discovery and characterization of novel non-substrate and substrate NAMPT inhibitors. *Mol Cancer Ther.* **16(7)**, 1236-1245.

33. Zabka, T. S., Singh, J., Dhawan, P., Liederer, B. M., Oeh, J., Kauss, M. A., Xiao, Y., Zak, M., Lin, T., McCray, B., *et al*. (2015). Retinal toxicity, in vivo and in vitro, associated with inhibition of nicotinamide phosphoribosyltransferase. *Toxicological Sciences* **144(1)**, 163–172.

Table 1. Exposure and vision assay results for 7 NAMPT inhibitors. The highest dose for each compound was the maximum tolerated dose.

			Startle Response (%)		Optomotor Response	
Compound	Dose (μM)	pmoles per larva	SOUND	LIGHT	Score	%
A-1343741	1	1.42	124	213	FAIL	44.4
	3	4.30	89	122	FAIL	11.7
	10	9.12	52	0	FAIL	10.6
A-1466391	0.3	0.35	323	112	FAIL	51.4
	1	0.72	258	228	FAIL	22.7
	3	2.11	133	0	FAIL	3.0
A-1325236	3	1.36	83	108	PASS	62.5
	10	1.97	81	128	PASS	66.7
	30	6.81	25	64	FAIL	45.8
A-1459319	1	1.53	104	190	FAIL	37.9
	3	2.08	56	19	FAIL	16.7
	10	6.49	30	0	FAIL	5.0
A-1442928	1	0.91	5	3.1	FAIL	4.5
	3	2.30	31	0	FAIL	1.0
	10	9.43	37	0	FAIL	1.0
A-1293201	30	10.70	112	106.0	FAIL	43.9
	100	51.70	85	19.5	FAIL	27.3
	300	119.00	413	0	FAIL	15.3
A-1326133	3	2.86	105	34.0	FAIL	29.2
	10	2.97	30	5.2	FAIL	16.7
	30	8.08	78	0	FAIL	21.2

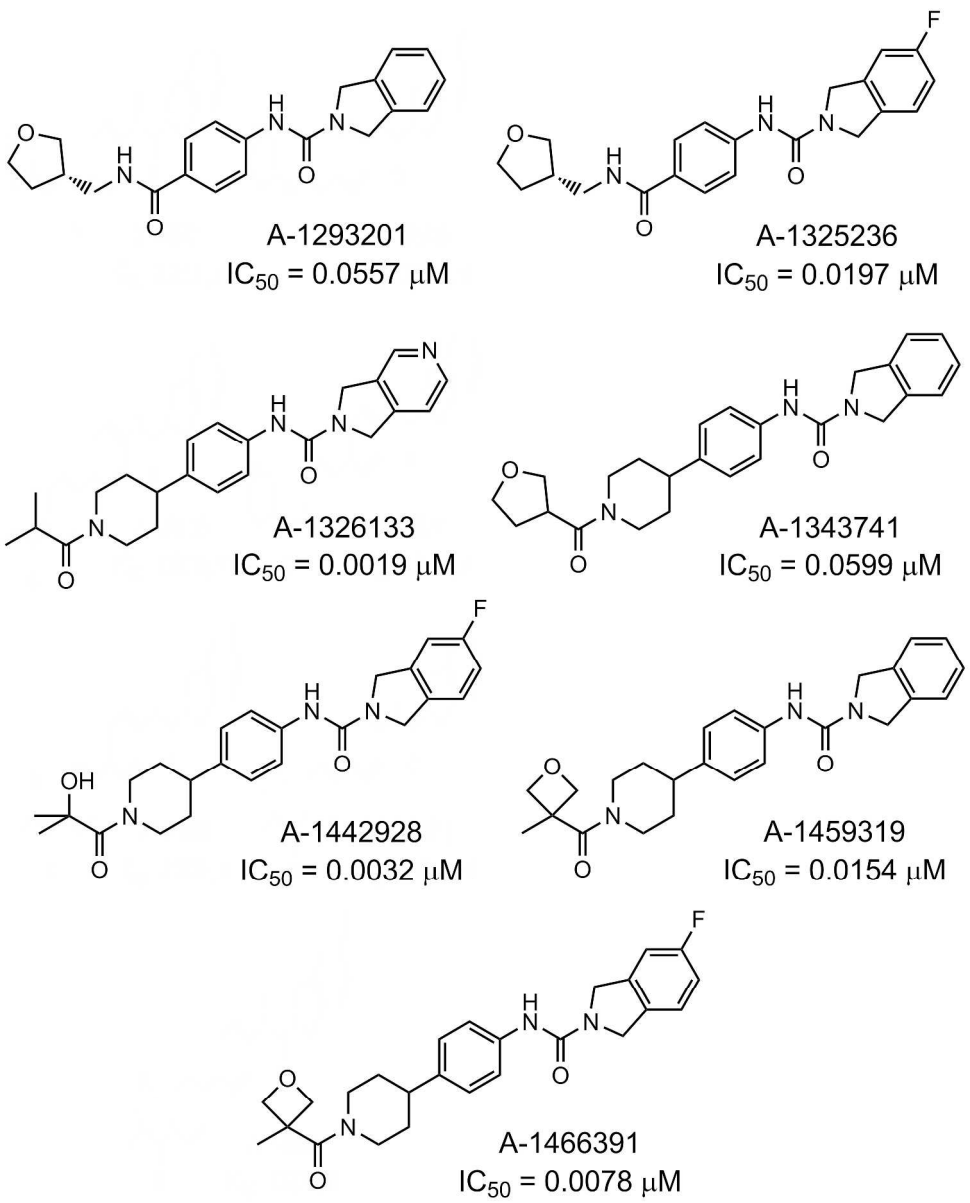

Fig. 1. Seven NAMPT inhibitors used for these studies. Structures are accompanied by the name and IC50 for inhibiting human PC3 tumor cells. Only A-1326133 is an azaisoindoline that is a substrate for NAMPT. All others are isoindoline non-substrate inhibitors of NAMPT.

182x225mm (600 x 600 DPI)

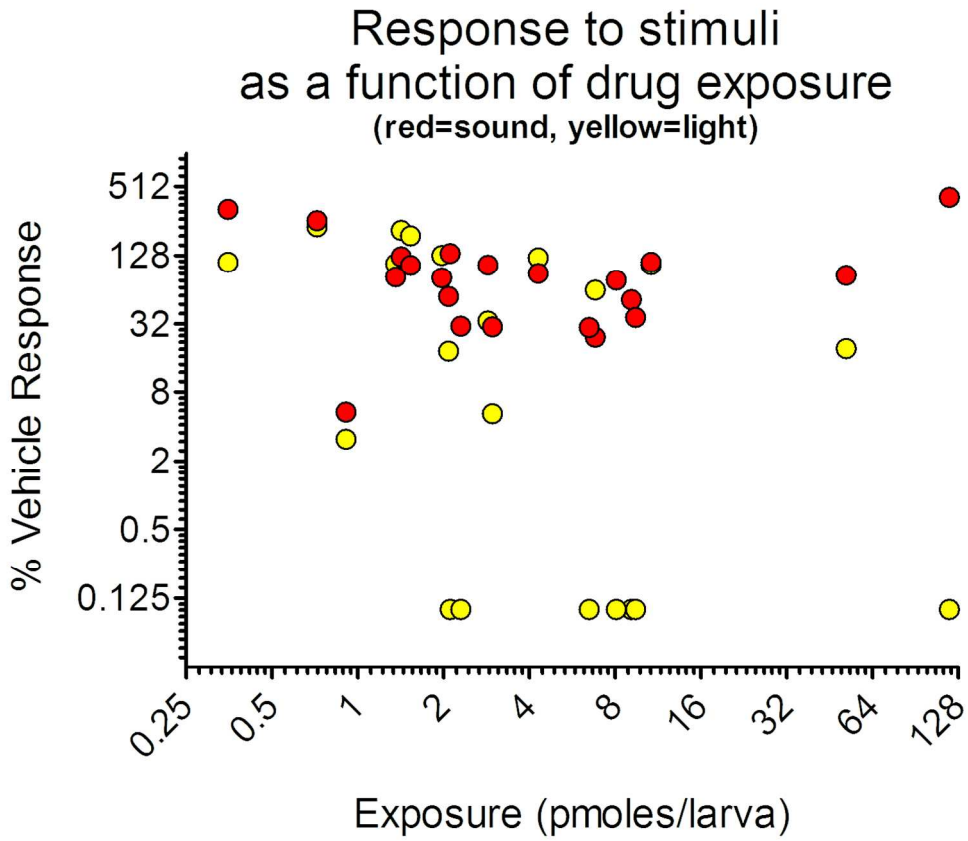

Fig. 2. Zebrafish response to sound or light stimulus as a function of exposure to NAMPT inhibitors. Results from 3 dose levels from each of the 7 compounds are provided for each stimulus. Each exposure (x-axis) is associated with paired data points, one for sound (red) and one for light (yellow). Note that where response to light is ablated (yellow symbols at bottom), response to sound often remained robust (red symbols corresponding to the same exposure), indicating loss of vision but not loss of hearing.

131x117mm (300 x 300 DPI)

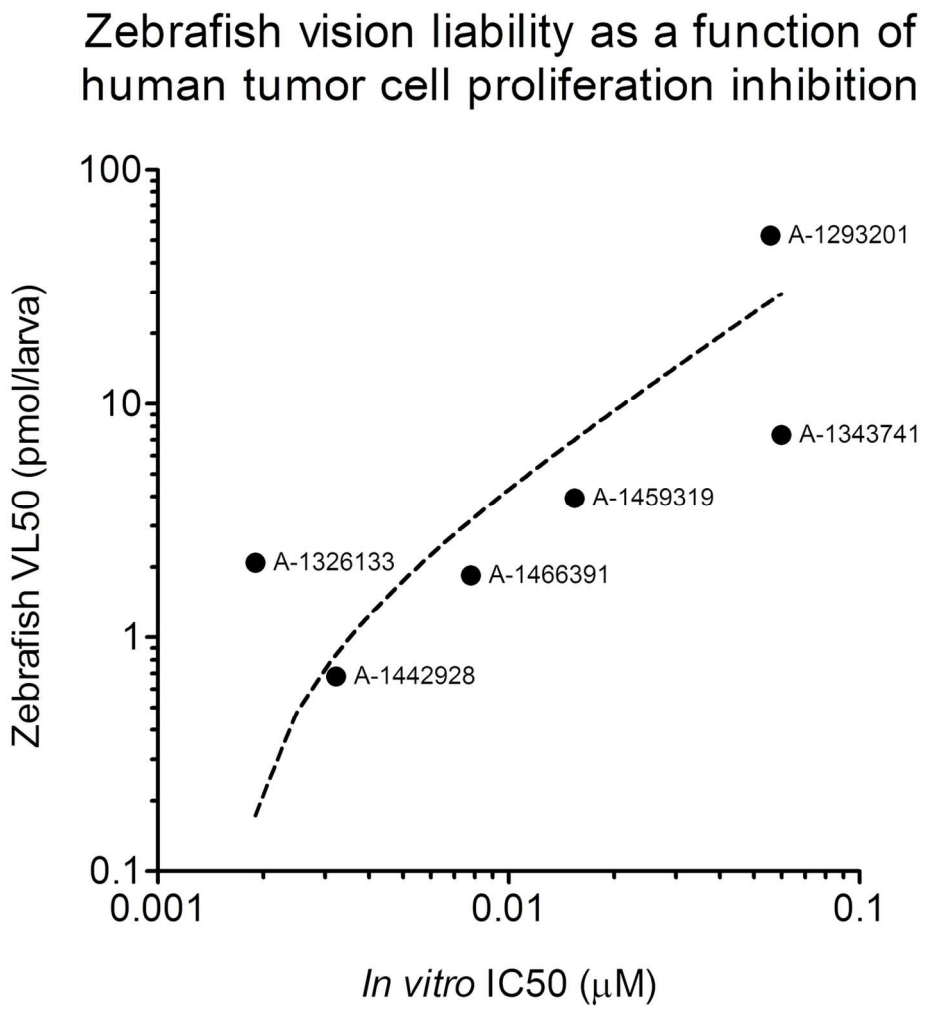

Fig. 3. Toxic potency on zebrafish vision for 6 NAMPT inhibitors as a function of potency to inhibit human PC3 tumor cell proliferation, R2 = 0.45. This correlation indicates translatable pharmacology of these compounds between zebrafish and human NAMPT.

135x142mm (300 x 300 DPI)

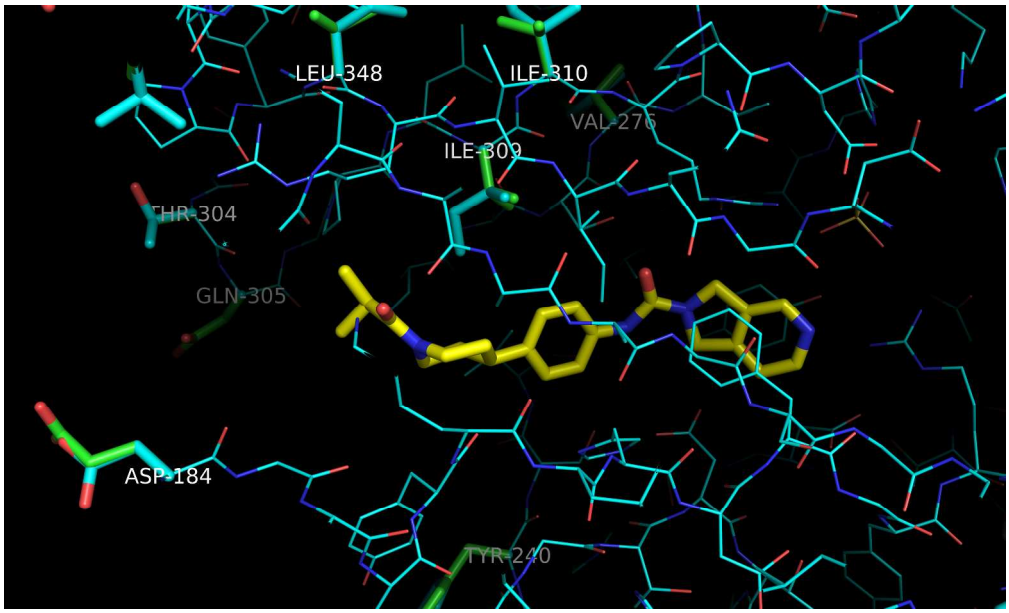

Fig. 4. Homology model of zebrafish and human NAMPT ligand binding sites. Amino acids of zebrafish NAMPT that are not homologous with those in the human NAMPT are highlighted in green on the crystal structure of human NAMPT (blue, pdb code 5U2N) complex with inhibitor A-1326133 (yellow). The structure of the ligand binding site is not predicted to be impacted by amino acid differences between zebrafish and human NAMPT.

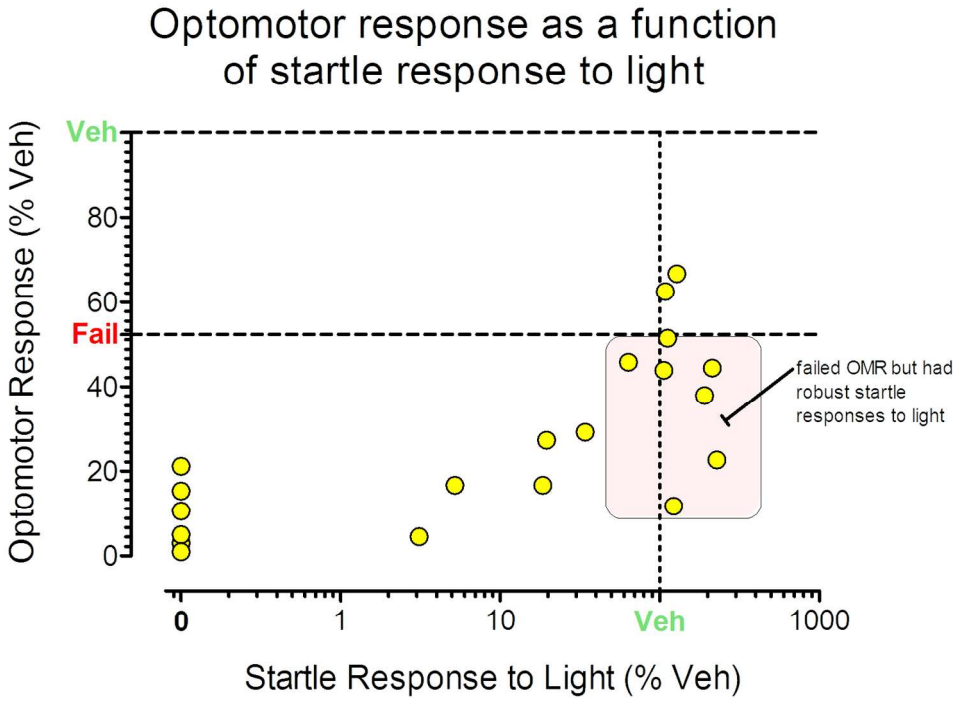

Fig. 5. Comparison of results for 2 zebrafish vision assays, the startle response to light and the optomotor response. Notice that some treatments resulting in a failed OMR result did not significantly impact startle response to light, as those same fish maintained > 50 % of vehicle treated response. This is indicative that OMR performance relies not only on vision, but also on sustained locomotion for the duration of the assay (18 minutes; 6 trials, 3 minutes each).

146x109mm (300 x 300 DPI)

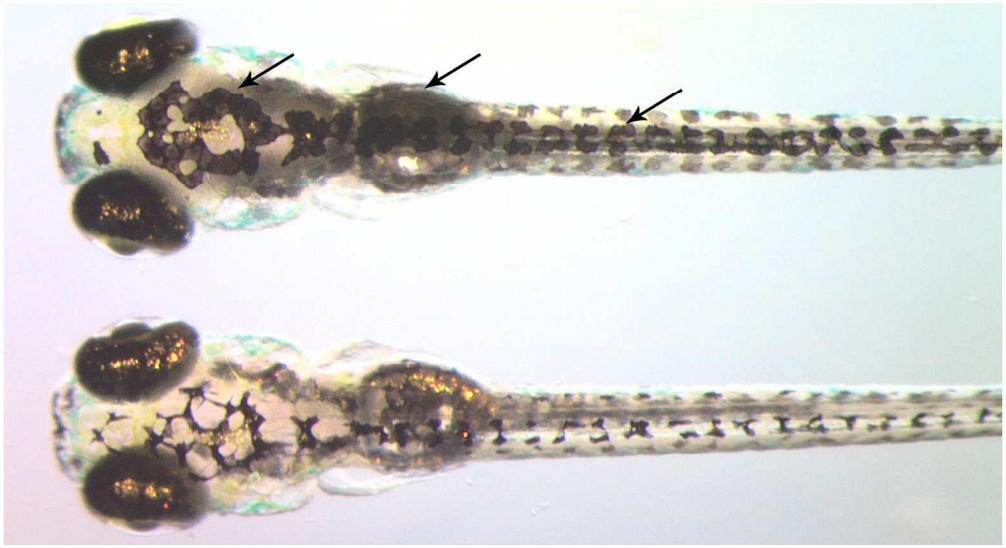

Fig. 6. Representative dorsal images of 8 dpf zebrafish larvae following a 72 hour treatment with (top) 10 μM A-1326133, or (bottom) vehicle. Increased visible melanin can indicate a visual deficit (perceived low/no light). The image was captured during lights-on when melanosomes are typically contracted in response to retinal signals; this is manifested in a lighter appearance, as observed in vehicle-treated fish (bottom). Arrows mark increased visible melanin in skin.

135x73mm (300 x 300 DPI)

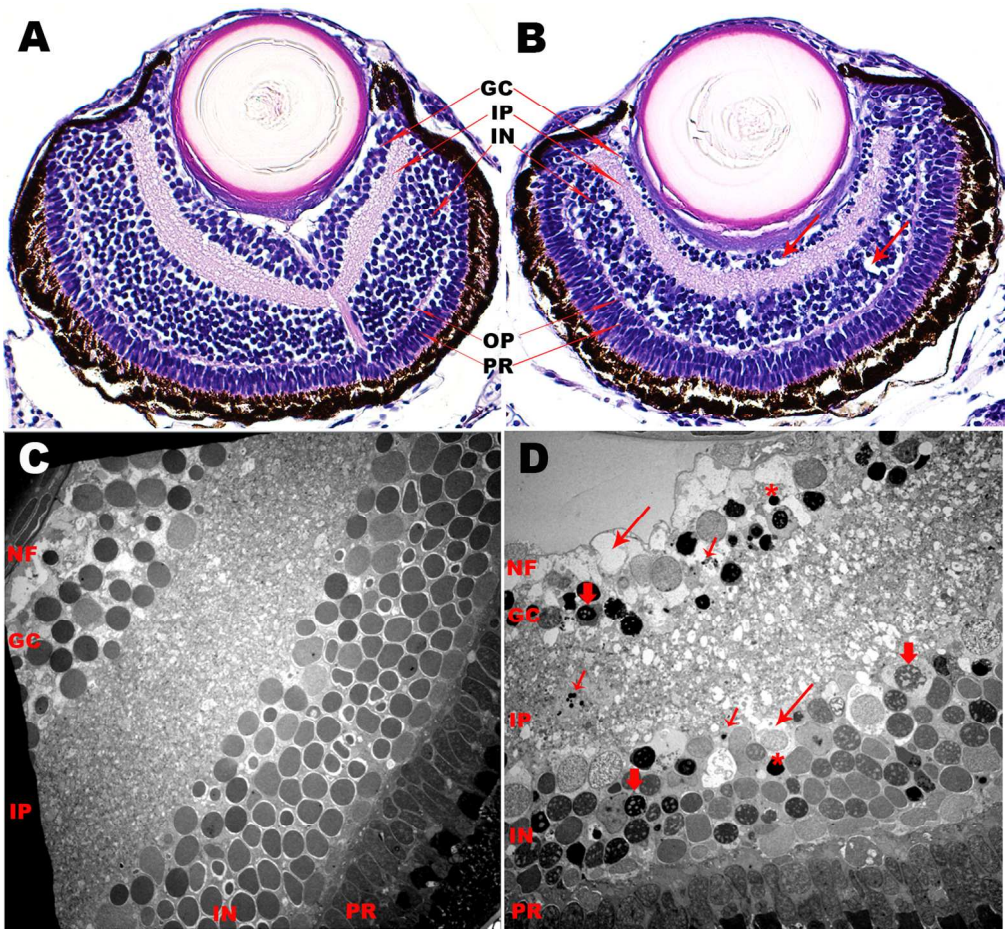

Fig. 7. Representative ocular histology (A, B) and electron microscopy (C, D) of 8 dpf zebrafish larvae following treatment with vehicle or NAMPT inhibitor (10 μM A-1326133). A and B, Histological transverse sections of eyes (40x). Vehicle treated eye (A) depicts normal retinal features for this stage of development. Note that at this stage, the outer plexiform layer is poorly developed. Decreased cell layers and numbers of nuclei present are depicted in the NAMPT inhibitor treated eye (B) in both the ganglion cell and inner nuclear layers (red arrows, right side of image). The inner plexiform layer has a disorganized, vacuolated appearance associated with cell loss in adjacent layers and their cell processes or axons. C and D, Transmission electron microscopy of zebrafish larvae retina (2000x). Vehicle treated retina (C) demonstrates normal features for developing larvae. Note the variably sized, relatively homogenous appearance of the nuclei in the ganglion and inner nuclear layers. In contrast, in the NAMPT inhibitor treated eye (D), many of the nuclei show evidence of apoptosis including nuclear pyknosis and condensation (red asterisk) and nuclear vacuolation and fragmentation (red block arrows). Apoptotic bodies (granular, electron dense, nuclear remnants) are present in both the ganglion and inner nuclear cell layer (red arrows). Vacuolation, or clear spaces (red arrows), are observed in the nerve fiber, ganglion cell, inner plexiform and inner nuclear layers associated with cell loss. NF = nerve fiber layer; GC = ganglion cell layer; IP = inner plexiform layer; IN = inner nuclear layer; OP = outer plexiform layer; PR = photoreceptor layer.

136x125mm (300 x 300 DPI)

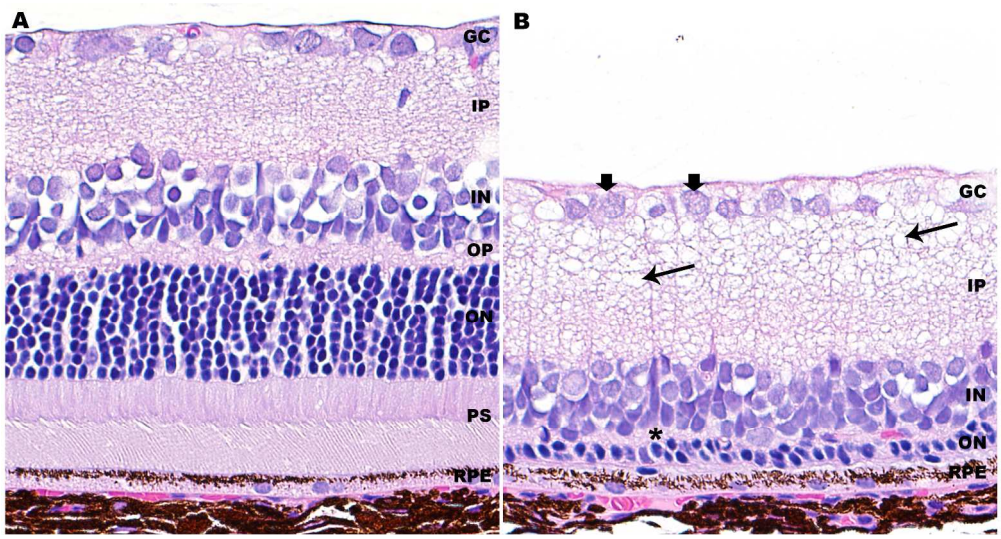

Fig. 8. Representative microscopic images of Long Evans rat retinas following treatment with (A) vehicle, Avicel CL-611 (1 ml/kg) and (B) NAMPT inhibitor, A-1326133 (10 mg/kg). Treatments were administered orally, once a day, starting at 8 weeks of age (4 days on, 3 days off, and 4 days on treatment). A, Treatment with vehicle resulted in no apparent retinal toxicity. B, A-1326133 induced retinal toxicity characterized by pronounced loss of photoreceptor nuclei (ON reduced to a single layer) with complete loss of photoreceptor segments; loss and collapse of the outer plexiform layer (remnant denoted by *); and rarefaction and vacuolation of the inner plexiform layer associated with loss of axons and cell processes (arrows). Ganglion cells appear to have diminished Nissl bodies and loss of nuclear detail (block arrows). Images taken at similar locations within the retina (H&E, 40x). GC = ganglion cell and nerve fiber layer; IP = inner plexiform layer; IN = inner nuclear layer; OP = outer plexiform layer; ON = outer nuclear layer; PS = photoreceptor segment layer; RPE = retinal pigmented epithelium.

284x151mm (300 x 300 DPI)